Chemistry & Biology
Article

A Genetically Encoded Metabolite Sensor for Malonyl-CoA

Jessica M. Ellis[1] and Michael J. Wolfgang[1,*]
[1]Department of Biological Chemistry, Johns Hopkins University School of Medicine, Baltimore, MD 21205, USA
*Correspondence: mwolfga1@jhmi.edu
http://dx.doi.org/10.1016/j.chembiol.2012.08.018

SUMMARY

Malonyl-CoA is the rate-determining metabolite for long chain de novo fatty acid synthesis and allosterically inhibits the rate-setting step in long chain fatty acid β-oxidation. We developed a cell-based genetically encoded biosensor based on the malonyl-CoA responsive *Bacillus subtilis* transcriptional repressor, FapR, for living mammalian cells. Here, we show that fluctuations in malonyl-CoA, in mammalian cells, can regulate the transcription of a FapR-based malonyl-CoA biosensor. The biosensor reflects changes in malonyl-CoA flux regulated by malonyl-CoA decarboxylase and AMP-activated protein kinase in a concentration-dependent manner. To gain further insight into the regulatory mechanisms that affect fatty acid metabolism, we used the malonyl-CoA sensor to screen and identify several kinases. LIMK1 was identified and its expression was shown to alter both fatty acid synthesis and oxidation rates. This simple genetically encoded biosensor can be used to study the metabolic properties of live mammalian cells and enable screens for novel metabolic regulators.

INTRODUCTION

Metabolite analysis has been largely confined to laborious measurements of whole tissues or populations of cells which gives an incomplete picture of a presumably intimate metabolic cross talk between cells. The elusive nature of cellular metabolites is due mainly to their relatively low abundance and short-lived nature. Furthermore, most intermediary metabolites have a simple structure that although functionally distinct, precludes the generation of specific antibodies or stains. A simple cell-based assay is needed to explore tissue metabolic heterogeneity and to perform high throughput screens to identify modifiers of important metabolic pathways.

One of the central metabolic pathways in biology is the synthesis of saturated long chain fatty acids. Fatty acids are used for membrane biosynthesis, the production of signaling lipids, post-translational modification (e.g., palmitoylation), energy storage and energy production. The rate of de novo fatty acid synthesis is largely controlled by the highly regulated acetyl-CoA carboxylase (ACC), which carboxylates cytoplasmic acetyl-CoA to malonyl-CoA (Figure 1A). Malonyl-CoA is then used as the chain-elongating unit for the synthesis of long chain fatty acids. Cytoplasmic malonyl-CoA also regulates fatty acid oxidation by allosterically inhibiting carnitine palmitoyltransferase-1, the rate-determining step in mitochondrial long chain fatty acid beta-oxidation. Therefore, malonyl-CoA is the regulatory link between the synthesis and oxidation of long chain fatty acids. While others have adapted bacterial proteins to generate unique FRET sensors for glutamate (Okumoto, et al., 2005), various carbohydrates (Fehr, et al., 2002, 2003, 2004, 2005; Lager, et al., 2003, 2006), citrate (Ewald, et al., 2011) and nucleotides (Berg, et al., 2009), there are a dearth of tools available to study fatty acid metabolism.

In gram positive bacteria, the synthesis of saturated fatty acids is transcriptionally regulated by the fatty acid and phospholipid regulator (FapR) (Schujman, et al., 2003). FapR is a transcriptional repressor that inhibits transcription of most genes involved in the fatty acid biosynthetic pathway. FapR undergoes a conformational shift when bound by malonyl-CoA that releases it from its operator (Kd = 2.4 μM), thereby allowing transcription of fatty acid biosynthetic genes (Schujman, et al., 2006). Therefore, these bacteria utilize malonyl-CoA as a concentration-dependent DNA binding inhibitor. The specificity of this interaction has been further validated by the crystallization of FapR bound to malonyl-CoA (Schujman, et al., 2006).

Here, we have produced a simple genetically encoded biosensor for mammalian cells that takes advantage of the malonyl-CoA dependent DNA binding properties of FapR. The biosensor is transcriptionally regulated by malonyl-CoA, thus reporter gene activity is correlated with the concentration of malonyl-CoA. We used the malonyl-CoA biosensor for a small scale expression screen to discover and validate kinases that regulate fatty acid metabolism. This simple malonyl-CoA biosensor design can be used to study the metabolic properties of live mammalian cells and enable screens to discover unknown metabolic regulators.

RESULTS AND DISCUSSION

Generation of a Mammalian Malonyl-CoA Sensor

We have adapted the bacterial FapR transcriptional regulatory system to generate a cell-based biosensor that can be used to detect changes in malonyl-CoA in mammalian cells. FapR, from *Bacillus subtilis* was codon optimized and synthesized for mammalian expression. FapR was then cloned into a mammalian expression vector and fused in-frame with the herpes simplex virus transcriptional activator, VP16. The VP16 fusion converts FapR from a bacterial transcriptional repressor into a transcriptional activator in the absence of malonyl-CoA. The 34 base pair fragment from the FapR operon (FapO) that is

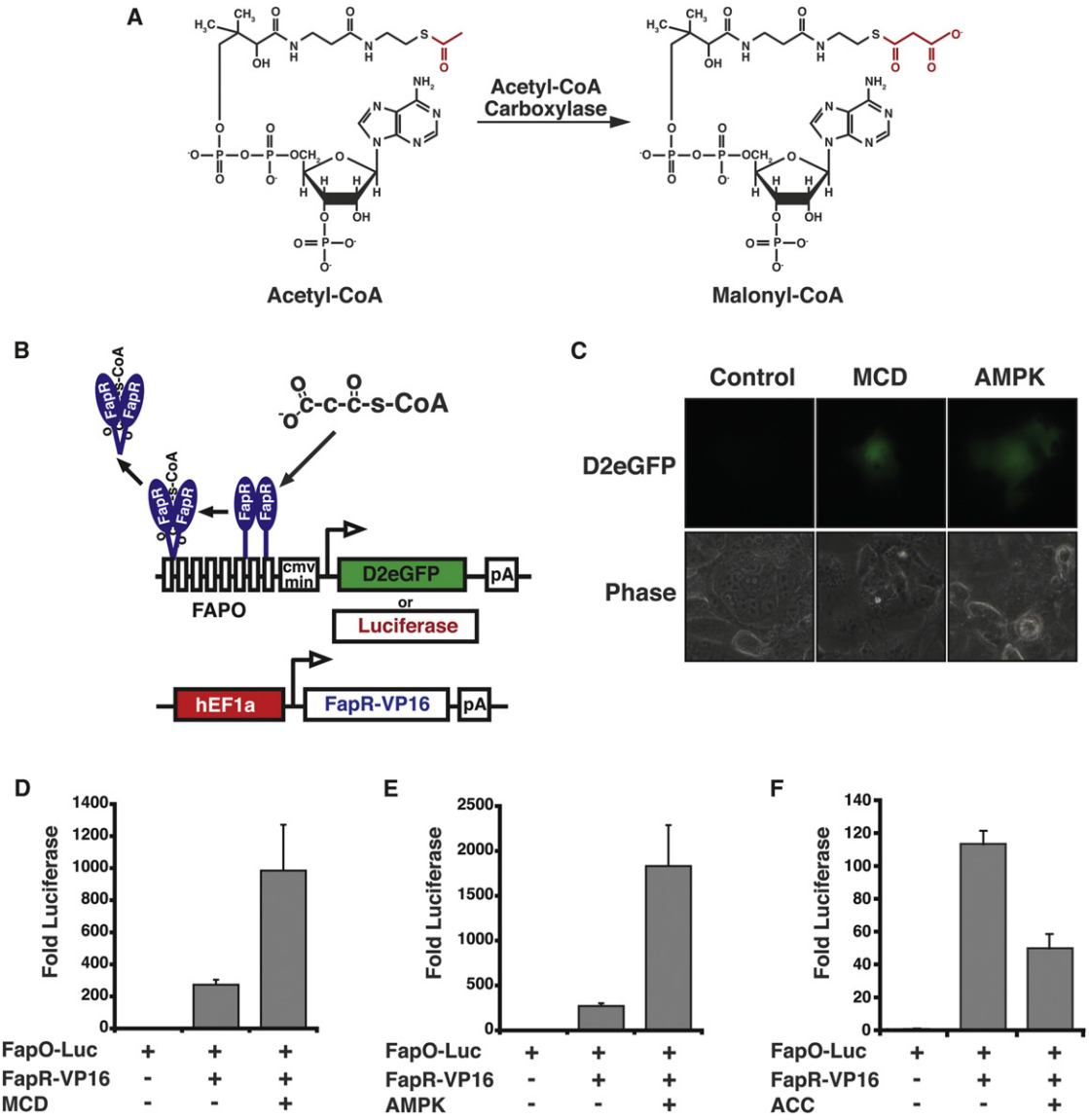

Figure 1. Development of a Genetically Encoded Malonyl-CoA Sensor

(A) The structurally similar but functionally distinct acetyl-CoA and malonyl-CoA.

(B) Schematic of the genetically encoded sensor based on the *Bacillus subtilis* transcriptional regulator, FapR.

(C) Depletion of malonyl-CoA by expression of a cytoplasmically targeted MCD or inhibiting the synthesis of malonyl-CoA by expression of a constitutively active AMPKgamma (R70Q) (AMPK) induces the expression of the destablized eGFP (D2eGFP) reporter or (D and E) luciferase reporter.

(D–F) The y axis shows the fold increase of luciferase luminescence normalized to beta-galactosidase activity relative to FapO-Luc alone. Error bars represent the standard error of the mean.

protected from DNase digestion by FapR binding was multerimized with a short linker and cloned upstream of a CMV minimal promoter driving either luciferase or a destabilized short half-life (~2 hr) green fluorescent protein (D2eGFP) (Figure 1B). The CMV minimal promoter provides the basic promoter elements including the TATA box and transcription initiation, but is relatively inert in the absence of an enhancer (Figures 1D–1F).

Next we wanted to validate that the malonyl-CoA biosensor was transcriptionally responsive to malonyl-CoA in mammalian cells. We were able to successfully co-express FapR-VP16 and the FapO-D2eGFP or FapO-Luciferase reporter in COS-1 cells (Figures 1C–1F). To validate the sensor, the concentration of cellular malonyl-CoA was altered in cells expressing the reporter plasmids by co-expressing enzymes that affect the concentration of malonyl-CoA. Co-expression of a cytoplasmically targeted malonyl-CoADecarboxylase (MCD) to catabolize malonyl-CoA to acetyl-CoA and CO_2 and lower cellular malonyl-CoA content (An, et al., 2004; Hu, et al., 2005; Rodriguez and Wolfgang, 2012) resulted in increased reporter fluorescence (Figure 1C) or luminescence (Figure 1D). Additionally, we co-expressed a constitutively active 5′-AMP-activated protein kinase-γ1 (R70Q) subunit (AMPK) (Hamilton, et al., 2001), to inhibit ACC and

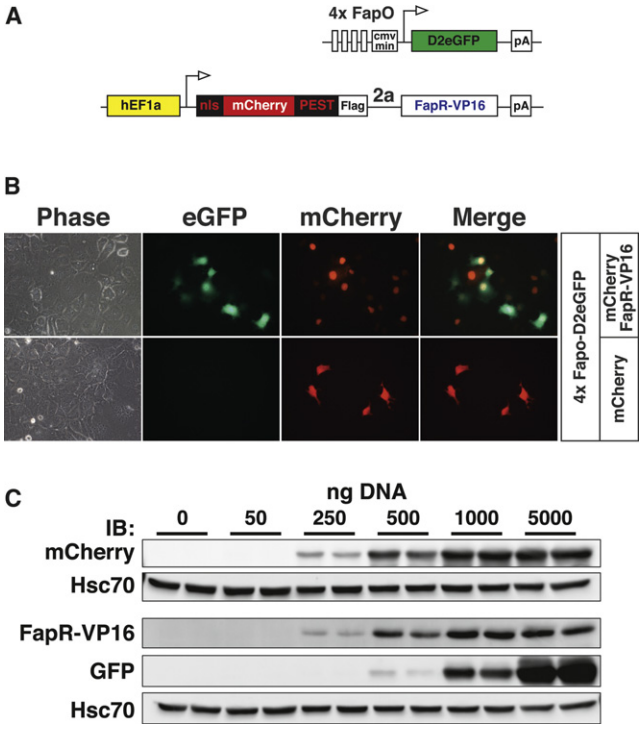

Figure 2. Fluorescent Malonyl-CoA Biosensor

(A) Schematic representation of the FapO-d2eGFP and nls-mCherry-PEST-Flag-2a-FapR-VP16 reporters.

(B) Phase contrast bright field, or epifluorescent eGFP, mCherry, and merge overlay images (40X magnification) of COS-1 cells transfected with the FapO-eGFP and mCherry-FapR-VP16 (top panel) or FapO-eGFP and mCherry reporter constructs.

(C) Western blot images of COS-1 cells cotransfected with increasing equimolar amounts of the FapO-eGFP reporter plasmid and nls-mCherry-PEST-Flag-2a-FapR-VP16 from 0 to 5000 ng DNA of each, and probed for anti-FLAG (representing the NLS-mCherry-PEST-FLAG), anti-VP16 (representing FapR-VP16), GFP, and the housekeeping protein HSC70.

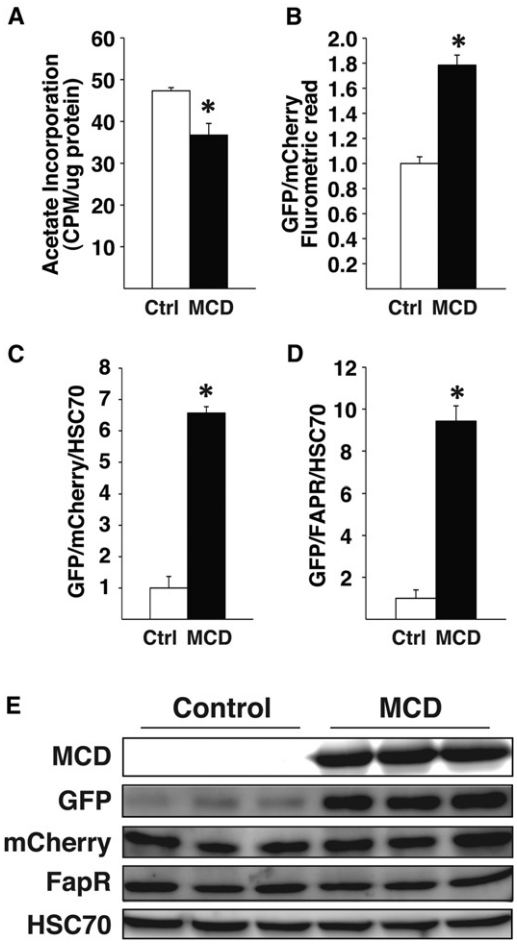

Figure 3. Malonyl-CoA Biosensor Altered by Depleting Cellular Malonyl-CoA

(A) [^{3}H]acetate incorporation into lipids.

(B) Fluorometric reading of GFP relative to mCherry.

(C–E) GFP protein abundance relative to mCherry or (D) FapR-VP16 protein abundance normalized to HSC70 housekeeping protein that was quantified from western blot images in (E). Western blot was probed with antibodies directed against V5 (MCD), GFP, FLAG (mCherry), VP16 (FapR-VP16), or HSC70 from COS-1 cells plated in 60 mm dishes and cotransfected with 50 ng of FapO-eGFP, 50 ng of mCherry-FapR-VP16, and 500 ng of either control (ctrl) or MCD expressing plasmid DNA. *$p < 0.05$, by Student's t test. Error bars represent the standard error of the mean. Western blots were developed using fluorescent secondary antibodies and quantified via AlphaInnotech MultiImage III.

therefore malonyl-CoA synthesis, which resulted in increased reporter fluorescence (Figure 1C) or luminescence (Figure 1E). Alternatively, the cotransfection of ACC1, to increase cellular malonyl-CoA, suppressed luciferase reporter activity (Figure 1F).

The malonyl-CoA sensor signal depends on both transfection efficiency and transcriptional activity of the cells; therefore, we modified the FapR-VP16 construct to include a destabilized mCherry fluorescent protein to control for both transfection and stability (Figure 2A). A picornavirus PTV1-2A peptide-linked destabilized mCherry was fused in-frame before FapR-VP16. The 2A peptide allows two proteins to be produced from a single mRNA at a 1:1 stoichiometric ratio, enabling a ratiometric, autonomous measurement of transfection within cells (Rodriguez and Wolfgang, 2012; Szymczak, et al., 2004). To enable a comparison between mCherry and destabilized eGFP, the PEST sequence from ornithine decarboxylase (also used in D2eGFP) was fused to mCherry along with a nuclear localization sequence (nls) to better visualize the transgene (Figure 2A). Images of the nuclear localized-fluorophore labeled FapR construct are shown in transfected COS-1 cells (Figure 2B). As in Figures 1D–1F, in the absence of FapR-VP16 there is minimal expression of the reporter, but the addition of FapR-VP16, as visualized by mCherry expression, greatly enhances eGFP expression (Figure 2B). Increasing transfection of each plasmid into COS-1 cells demonstrated an increase in both the GFP and mCherry fluorescent signal as expected (Figure 2C).

Dynamics of the Malonyl-CoA Biosensor

To verify that the malonyl-CoA biosensor can determine relative qualitative differences in malonyl-CoA in living mammalian cells, we expressed MCD in COS-1 cells and measured [^{3}H]acetate incorporation into lipids while simultaneously measuring reporter activity. The expression of MCD in COS-1 cells resulted in decreased [^{3}H]acetate incorporation into lipids as expected (Figure 3A). The malonyl-CoA reporter showed an increase in the

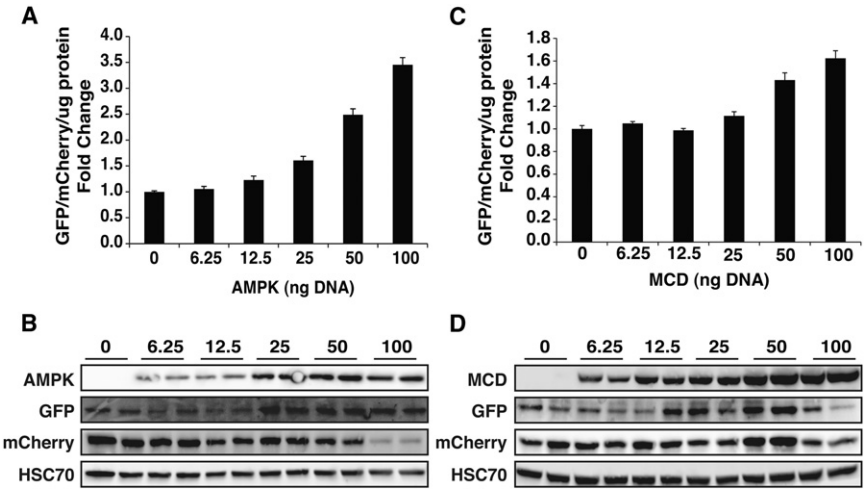

Figure 4. Malonyl-CoA Biosensor Titration

(A–D) GFP fluorescent quantification relative to mCherry fluorescence read in a fluorescent plate reader, normalized to protein, in COS-1 cells plated in 24-well plates and cotransfected with 5 ng FapO-eGFP reporter DNA, 50 ng nls-mCherry-PEST-Flag-2a-FapR-VP16, and increasing levels of constitutively active AMPK gamma (R70Q) DNA (A) or MCD DNA (C). Western blot images and quantification of COS-1 cells described above and probed against GFP, FLAG (mCherry), HSC70, and HA (AMPK) (B) or V5 (cMCD) (D).

GFP/mCherry ratio as measured by direct cellular fluorescence by a fluorometric platereader (Figure 3B). Subsequently, cell lysate was subjected to western blot analysis for detection of all transfected components (Figure 3E). Western blot densitometry showed a large increase in the ratio of GFP/mCherry (Figure 3C) and an even larger increase in the ratio of GFP/FapR (Figure 3D). While both fluorescent reading and western blot analysis similarly reflect biosensor activity, in our hands western blot analysis is a more sensitive measure than direct fluorescence reading. Given the laborious nature of western blot analysis, the convenience of direct fluorescence measurement makes fluorescence reading more desirable for initial screening and subsequent applications. The GFP/mCherry ratio is modest in comparison to the GFP/FapR ratio, accurately reflecting the short-lived nature of the destabilized mCherry and long-lived nature of the FapR-VP16.

Next, we expressed increasing concentrations of AMPK or MCD in COS-1 cells. AMPK phosphorylates and deactivates ACC thereby reducing malonyl-CoA flux through de novo fatty acid synthesis, and correspondingly we show that increasing the expression of exogenous AMPK increased the reporter fluorescence reading and protein abundance in a dose-dependent manner (Figures 4A and 4B). Likewise, increasing the expression of MCD, an enzyme that converts malonyl-CoA to acetyl-CoA, thereby depleting cellular malonyl-CoA, showed a dose-dependent increase in reporter fluorescence reading and protein abundance (Figures 4C and 4D). AMPK, while a robust inhibitor of ACC, also inhibits protein synthesis and augments autophagy (Kahn, et al., 2005) and thus affects the protein abundance of FapR-VP16 and mCherry but retains the expected GFP/mCherry ratio. These data show that modulating malonyl-CoA metabolizing enzymes induced the predicted changes in reporter activity of this genetically encoded malonyl-CoA biosensor.

Identifying Novel Mechanisms to Affect Malonyl-CoA Concentration

The enzymatic regulation of fatty acid synthetic and degradative pathways has been thoroughly examined (Wakil and Abu-Elheiga, 2009). However, the signaling mechanisms that translate extracellular cues into alterations in mammalian cellular metabolism are less clear. To gain mechanistic insight into how diverse signaling cascades regulate malonyl-CoA concentration, we used the reporter activity of the malonyl-CoA biosensor to screen a myristoylated human kinase expression library (Boehm, et al., 2007) in COS-1 cells (Figure 5A). AMPK was used as a positive control and the empty vector was used as a negative control. Several novel kinases were found that decreased reporter activity and thus increase malonyl-CoA concentration. We performed a secondary counter screen with or without MCD co-expression on a subset of seven kinases that changed reporter signal greater than 2-fold (Mapk7, Akt1, Map2K5, Prkra, LIMK1, MAPK13, and CSNK1A1L) and we found that the LIMK1, MAPK13, and CSNK1A1L kinases did appear to increase malonyl-CoA content because reporter activity was reversed with the expression of MCD (Figure 5B). Here, we have shown the FapR-based malonyl-CoA biosensor can be used to identify possible mediators of fatty acid metabolism.

Next, we chose to further validate the regulation of fatty acid metabolism by LIMK1. Decreased signal from the malonyl-CoA reporter induced by cotransfection with LIMK1 suggests an increase in metabolic flux through lipid synthesis and a simultaneous suppression of fatty acid beta-oxidation. To confirm that the sensor activity reflects changes in the flux of fatty acid biosynthesis, we performed the standard biochemical assay for de novo fatty acid synthesis, [^{3}H]acetate incorporation into lipids, on cells transfected with LIMK1. As expected, increasing concentrations of LIMK1 DNA increased the rate of de novo fatty acid synthesis (Figure 5C). This suggests that LIMK1 alters fatty acid metabolism consistent with the malonyl-CoA biosensor activity. The LIMK1-induced reduction in the malonyl-CoA sensor reflected an increase in the rate of cellular fatty acid synthesis. To further validate the malonyl-CoA sensor, we performed long chain fatty acid oxidation assays (by collecting ^3H_2O derived from the complete oxidation of [9,10 ^{3}H]palmitate) on COS-1 cells expressing carnitine palmitoyltransferase-1a (CPT1a), the rate-setting enzyme in fatty acid oxidation that is potently inhibited by cytoplasmic malonyl-CoA. As predicted, the rates of fatty acid oxidation were significantly decreased in the LIMK1 expressing COS-1-Cpt1a cells (Figure 5D), suggesting that LIMK1 increases malonyl-CoA thereby inhibiting CPT1a activity. LIMK1 has been shown to be critical for neurite outgrowth in vitro (Endo, et al., 2007). LIMK1 is linked to the regulation neurite extension through its regulation of cofilin, a regulator of actin cytoskeletal dynamics (Takemura, et al., 2009).

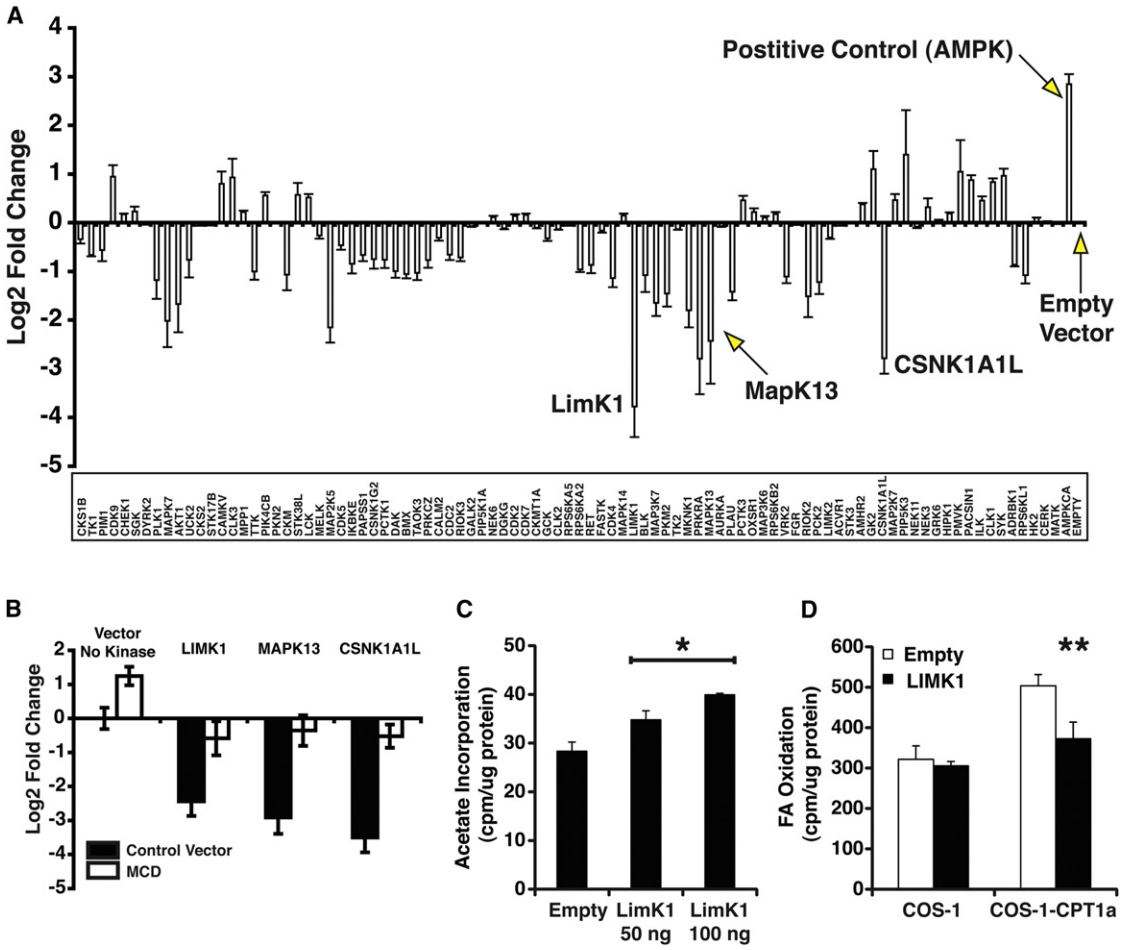

Figure 5. Identification of Novel Signaling Regulators of Fatty Acid Synthesis via Expression Screening

(A) COS-1 cells were cotransfected with the malonyl-CoA biosensor and 100 ng DNA of myristoylated kinase plasmids in quadruplicate. A constitutively active AMPK gamma (R70Q) was used as the positive control and an empty vector was used as the negative control.

(B) A subset of kinases that were identified in the screen were subjected to a secondary screen with or without MCD.

(C) COS-1 cells cotransfected with 100 ng LIMK1 DNA and sensor expression plasmids have increased de novo lipid synthesis assayed by the incorporation of ^{3}H-acetate into lipids.

(D) COS-1 cells with or without stable expression of carnitine palmitoyltransferase 1a (COS-1-CPT1a) (Reamy and Wolfgang, 2011) were cotransfected with a 100 ng LIMK1 and sensor expression plasmids. LIMK1 suppressed CPT1a-mediated oxidation of [9,10 ^{3}H]palmitic acid. *$p < 0.05$, **$p < 0.005$ by Student's t test. Error bars represent the standard error of the mean.

Here, we show that LIMK1 increases the rate of de novo fatty acid synthesis when expressed in COS-1 cells. While neurite extension most certainly requires cytoskeletal rearrangement, outgrowth may also require the formation of new fatty acids for the synthesis of phospholipids used for membrane extension. Our malonyl-CoA sensor kinase screen has revealed a role for LIMK1 in altering cellular fatty acid metabolic rates.

SIGNIFICANCE

We developed a genetically encoded biosensor for an important but elusive metabolite, malonyl-CoA. This simple methodology can be used to dissect cell-specific metabolic properties in complex tissues or can be used to perform screens to identify new modes of metabolic regulation. A limitation of our sensor is that the reporter signal relies upon the transcriptional and translational activity of the host cell and can only respond to nucleocytoplasmic metabolites. This is why counter screening, metabolite flux analysis using labeled substrates, or direct measurements of the metabolite are required as orthogonal measures to confirm that the effect is specific for a change in metabolite flux. Additionally, to obtain reliable reporter activity, both the reporter and activator need to be controlled for as we have shown.

FRET-based sensors have been very useful for determining the temporal and subcellular resolution of small molecules, but have been limited in their utility for large scale screening or in vivo use. The metabolite sensitive transcriptional reporters described here are analogous to the widely used tetracycline regulated transcriptional control that has been used extensively in vitro and in vivo (Lee, et al., 1998; Li, et al., 2005; Mayford, et al., 1996; Nguyen,

et al., 2006). **The use of bacterial-derived metabolite sensitive transcriptional reporters eliminates the requirement to overexpress endogenous enzymes or transcription factors, the requirement to modify the metabolite directly, and the requirement to modify endogenous metabolite generating or degrading enzymes. More broadly, bacteria encode a wealth of small molecule regulated transcription factors that could be similarly modified to understand equally onerous-to-study molecules.**

EXPERIMENTAL PROCEDURES

Constructs

A mammalian codon optimized FapR cDNA was synthesized and cloned as an N-terminal fusion protein to VP16 in a mammalian expression vector, pEF6 (Life Technologies). Additionally, DNA encoding a nuclear localization sequence, a PEST sequence, mCherry, FLAG, and the self-cleaving 2A peptide sequence were synthesized (Life Technologies) and inserted into the FapR-VP16 plasmid by In-fusion (Clontech, Mountain View, CA). A 34 base pair fragment of the FapR operon was PCR amplified and multimerized then cloned upstream to a CMV minimal promoter and firefly luciferase cDNA or a destabilized eGFP. Transfections were performed with Fugene HD at a microgram DNA to microliter Fugene ratio of 1:3 (Promega). For all transfections 50 ng each of FapR-VP16, FapO-GFP, and FapO-Luc expression plasmids were transfected, unless otherwise specified. Luciferase assays were normalized by cotransfection with CMV-βgal. Luciferase assays (Promega) were done in quadruplicate and normalized to beta galactosidase activity (Pierce) per manufacturer's instructions. The myristoylated human kinase library was obtained from Addgene (no.1000000012). Constructs for MCD were generated by PCR amplification of mouse skeletal muscle cDNA as previously published (An, et al., 2004). HA-tagged AMPKgamma (R70Q) plasmids (Hamilton, et al., 2001) have been previously described. A mammalian expression vector for ACC1 was purchased from Life Technologies.

De Novo Fatty Acid Synthesis

COS-1 cells transfected with a kinase expression plasmid were labeled with trace levels (1.0 μCi) of [^{3}H]acetic acid (Perkin Elmer) for 1 hr. Total lipids were extracted with chloroform/methanol via Folch method (Folch, et al., 1957) and radioactivity was counted via liquid scintillation.

Fatty Acid Oxidation

COS-1 cells or COS-1 cells expressing carnitine palmitoyltransferase 1a (CPT1a) (Reamy and Wolfgang, 2011) transfected with a kinase expression plasmid were incubated with BSA-conjugated [9,10 ^{3}H]palmitate (Perkin Elmer) for 2 hr. The media was acidified, precipitated, then neutralized, and ^3H_2O was isolated through ion exchange chromatography as previously reported and radioactivity was counted via liquid scintillation (Buzzai, et al., 2005).

Reporter Quantification

Fluorescent signal was measured by plate reader at 485 nm excitation and 528 nm emission for green fluorescence protein and 550 nm excitation and 610 nm emission for mCherry on a BioTek SynergyMx plate reader (Winooski, VT). The GFP signal was normalized to mCherry signal and values were normalized to the control treated cells. Western blots were quantified using Alpha Innotech FluorChem Q Software (Santa Clara, CA) in which 20 ug protein were loaded onto 8% SDS/polyacrylamide gels, transferred to nitrocellulose membranes and blocked with 5% non-fat dry milk in TBS-1% Tween-20. Primary antibodies were GFP (Santa Cruz sc-9996), FLAG (Agilent cat no. 200470-21), VP16 (Santa Cruz, sc-7545), V5 (Invitrogen P/N46-0705 Santa Cruz), HA (Roche cat no. 11867423001), and HSC70 (Santa Cruz, sc-7298).

ACKNOWLEDGMENTS

We would like to thank Violeta Capric (Wagner College) for technical assistance. J.M.E. was supported by an interdepartmental training program in cellular and molecular endocrinology (T32DK007751). This work was supported in part by the American Heart Association (SDG2310008 to M.J.W.) and NIH NINDS (NS072241 to M.J.W.).

Received: March 10, 2012
Revised: August 17, 2012
Accepted: August 23, 2012
Published: October 25, 2012

REFERENCES

An, J., Muoio, D.M., Shiota, M., Fujimoto, Y., Cline, G.W., Shulman, G.I., Koves, T.R., Stevens, R., Millington, D., and Newgard, C.B. (2004). Hepatic expression of malonyl-CoA decarboxylase reverses muscle, liver and whole-animal insulin resistance. Nat. Med. *10*, 268–274.

Berg, J., Hung, Y.P., and Yellen, G. (2009). A genetically encoded fluorescent reporter of ATP:ADP ratio. Nat. Methods *6*, 161–166.

Boehm, J.S., Zhao, J.J., Yao, J., Kim, S.Y., Firestein, R., Dunn, I.F., Sjostrom, S.K., Garraway, L.A., Weremowicz, S., Richardson, A.L., et al. (2007). Integrative genomic approaches identify IKBKE as a breast cancer oncogene. Cell *129*, 1065–1079.

Buzzai, M., Bauer, D.E., Jones, R.G., Deberardinis, R.J., Hatzivassiliou, G., Elstrom, R.L., and Thompson, C.B. (2005). The glucose dependence of Akt-transformed cells can be reversed by pharmacologic activation of fatty acid beta-oxidation. Oncogene *24*, 4165–4173.

Endo, M., Ohashi, K., and Mizuno, K. (2007). LIM kinase and slingshot are critical for neurite extension. J. Biol. Chem. *282*, 13692–13702.

Ewald, J.C., Reich, S., Baumann, S., Frommer, W.B., and Zamboni, N. (2011). Engineering genetically encoded nanosensors for real-time in vivo measurements of citrate concentrations. PLoS ONE *6*, e28245.

Fehr, M., Frommer, W.B., and Lalonde, S. (2002). Visualization of maltose uptake in living yeast cells by fluorescent nanosensors. Proc. Natl. Acad. Sci. USA *99*, 9846–9851.

Fehr, M., Lalonde, S., Lager, I., Wolff, M.W., and Frommer, W.B. (2003). In vivo imaging of the dynamics of glucose uptake in the cytosol of COS-7 cells by fluorescent nanosensors. J. Biol. Chem. *278*, 19127–19133.

Fehr, M., Lalonde, S., Ehrhardt, D.W., and Frommer, W.B. (2004). Live imaging of glucose homeostasis in nuclei of COS-7 cells. J. Fluoresc. *14*, 603–609.

Fehr, M., Takanaga, H., Ehrhardt, D.W., and Frommer, W.B. (2005). Evidence for high-capacity bidirectional glucose transport across the endoplasmic reticulum membrane by genetically encoded fluorescence resonance energy transfer nanosensors. Mol. Cell. Biol. *25*, 11102–11112.

Folch, J., Lees, M., and Sloane Stanley, G.H. (1957). A simple method for the isolation and purification of total lipides from animal tissues. J. Biol. Chem. *226*, 497–509.

Hamilton, S.R., Stapleton, D., O'Donnell, J.B., Jr., Kung, J.T., Dalal, S.R., Kemp, B.E., and Witters, L.A. (2001). An activating mutation in the gamma1 subunit of the AMP-activated protein kinase. FEBS Lett. *500*, 163–168.

Hu, Z., Dai, Y., Prentki, M., Chohnan, S., and Lane, M.D. (2005). A role for hypothalamic malonyl-CoA in the control of food intake. J. Biol. Chem. *280*, 39681–39683.

Kahn, B.B., Alquier, T., Carling, D., and Hardie, D.G. (2005). AMP-activated protein kinase: ancient energy gauge provides clues to modern understanding of metabolism. Cell Metab. *1*, 15–25.

Lager, I., Fehr, M., Frommer, W.B., and Lalonde, S. (2003). Development of a fluorescent nanosensor for ribose. FEBS Lett. *553*, 85–89.

Lager, I., Looger, L.L., Hilpert, M., Lalonde, S., and Frommer, W.B. (2006). Conversion of a putative Agrobacterium sugar-binding protein into a FRET sensor with high selectivity for sucrose. J. Biol. Chem. *281*, 30875–30883.

Lee, P., Morley, G., Huang, Q., Fischer, A., Seiler, S., Horner, J.W., Factor, S., Vaidya, D., Jalife, J., and Fishman, G.I. (1998). Conditional lineage ablation to model human diseases. Proc. Natl. Acad. Sci. USA *95*, 11371–11376.

Li, X.D., Sun, L., Seth, R.B., Pineda, G., and Chen, Z.J. (2005). Hepatitis C virus protease NS3/4A cleaves mitochondrial antiviral signaling protein off the

mitochondria to evade innate immunity. Proc. Natl. Acad. Sci. USA *102*, 17717–17722.

Mayford, M., Bach, M.E., Huang, Y.Y., Wang, L., Hawkins, R.D., and Kandel, E.R. (1996). Control of memory formation through regulated expression of a CaMKII transgene. Science *274*, 1678–1683.

Nguyen, H., Rendl, M., and Fuchs, E. (2006). Tcf3 governs stem cell features and represses cell fate determination in skin. Cell *127*, 171–183.

Okumoto, S., Looger, L.L., Micheva, K.D., Reimer, R.J., Smith, S.J., and Frommer, W.B. (2005). Detection of glutamate release from neurons by genetically encoded surface-displayed FRET nanosensors. Proc. Natl. Acad. Sci. USA *102*, 8740–8745.

Reamy, A.A., and Wolfgang, M.J. (2011). Carnitine palmitoyltransferase-1c gain-of-function in the brain results in postnatal microencephaly. J. Neurochem. *118*, 388–398.

Rodriguez, S., and Wolfgang, M.J. (2012). Targeted chemical-genetic regulation of protein stability in vivo. Chem. Biol. *19*, 391–398.

Schujman, G.E., Paoletti, L., Grossman, A.D., and de Mendoza, D. (2003). FapR, a bacterial transcription factor involved in global regulation of membrane lipid biosynthesis. Dev. Cell *4*, 663–672.

Schujman, G.E., Guerin, M., Buschiazzo, A., Schaeffer, F., Llarrull, L.I., Reh, G., Vila, A.J., Alzari, P.M., and de Mendoza, D. (2006). Structural basis of lipid biosynthesis regulation in Gram-positive bacteria. EMBO J. *25*, 4074–4083.

Szymczak, A.L., Workman, C.J., Wang, Y., Vignali, K.M., Dilioglou, S., Vanin, E.F., and Vignali, D.A. (2004). Correction of multi-gene deficiency in vivo using a single 'self-cleaving' 2A peptide-based retroviral vector. Nat. Biotechnol. *22*, 589–594.

Takemura, M., Mishima, T., Wang, Y., Kasahara, J., Fukunaga, K., Ohashi, K., and Mizuno, K. (2009). Ca2+/calmodulin-dependent protein kinase IV-mediated LIM kinase activation is critical for calcium signal-induced neurite outgrowth. J. Biol. Chem. *284*, 28554–28562.

Wakil, S.J., and Abu-Elheiga, L.A. (2009). Fatty acid metabolism: target for metabolic syndrome. J. Lipid Res. Suppl. *50*, S138–S143.